JOURNAL OF TISSUE ENGINEERING AND REGENERATIVE MEDICINE
J Tissue Eng Regen Med (2015)
Published online in Wiley Online Library (wileyonlinelibrary.com) **DOI:** 10.1002/term.2092

RESEARCH ARTICLE

Posterior talar process as a suitable cell source for treatment of cartilage and osteochondral defects of the talus

S. I. Correia[1,2], J. Silva-Correia[1,2], H. Pereira[1,2,3,4], R. F. Canadas[1,2], A. da Silva Morais[1,2], A. M. Frias[1,5], R. A. Sousa[1,5], C. N. van Dijk[3,6], J. Espregueira-Mendes[1,2,3], R. L. Reis[1,2] and J. M. Oliveira[1,2]*

[1]*3Bs Research Group, Biomaterials, Biodegradables and Biomimetics, University of Minho, Headquarters of the European Institute of Excellence on Tissue Engineering and Regenerative Medicine, AvePark 4805-017, Barco, Guimarães, Portugal*
[2]*ICVS/3Bs, PT Government Associate Laboratory, Braga/Guimarães, Portugal*
[3]*Clínica do Dragão - Espregueira-Mendes Sports Centre - FIFA Medical Centre of Excellence, F.C. Porto Stadium, Minho University and Porto University Research Centre, Portugal*
[4]*Orthopaedic Department Centro Hospitalar Póvoa de Varzim, Vila do Conde, Portugal*
[5]*Stemmatters, Biotecnologia e Medicina Regenerativa SA, 4805-017, Guimarães, Portugal*
[6]*Orthopaedic Department, Amsterdam Medical Centre, The Netherlands*

Abstract

Osteochondral defects of the ankle are common lesions affecting the talar cartilage and subchondral bone. Current treatments include cell-based therapies but are frequently associated with donor-site morbidity. Our objective is to characterize the posterior process of the talus (SP) and the os trigonum (OT) tissues and investigate their potential as a new source of viable cells for application in tissue engineering and regenerative medicine. SP and OT tissues obtained from six patients were characterized by micro-computed tomography and histological, histomorphometric and immunohistochemical analyses. Proliferation and viability of isolated cells were evaluated by MTS assay, DNA quantification and live/dead staining. The TUNEL assay was performed to evaluate cell death by apoptosis. Moreover, the production of extracellular matrix was evaluated by toluidine blue staining, whereas cells phenotype was investigated by flow cytometry. Characterization of ankle explants showed the presence of a cartilage tissue layer in both SP and OT tissues, which represented at least 20%, on average, of the explant. The presence of type II collagen was detected in the extracellular matrix. Isolated cells presented a round morphology typical of chondrocytes. In *in vitro* studies, cells were viable and proliferating for up to 21 days of culture. No signs of apoptosis were detected. Flow-cytometry analysis revealed that isolated cells maintained the expression of several chondrocytic markers during culture. The results indicated that the SP and OT tissues were a reliable source of viable chondrocytes, which could find promising applications in ACI/MACI strategies with minimal concerns regarding donor zone complications. Copyright © 2015 John Wiley & Sons, Ltd.

Received 26 June 2015; Accepted 9 September 2015

Keywords **ankle; osteochondral lesions; os trigonum; regenerative medicine; Stieda process; talus lesions**

1. Introduction

Osteochondral defects (OCDs) of the ankle represent 4% of all osteochondral lesions in the body (Reddy *et al.*, 2007). Ankle OCDs affecting both the talar cartilage and subchondral bone are mostly caused by single or multiple traumatic events. These types of lesions frequently progress to partial or complete detachment of the fragment, causing deep ankle pain, especially if associated with

**Correspondence to: Joaquim M. Oliveira, 3Bs Research Group, Biomaterials, Biodegradables and Biomimetics, University of Minho, Headquarters of the European Institute of Excellence on Tissue Engineering and Regenerative Medicine, AvePark, Parque de Ciência e Tecnologia, Zona Industrial da Gandra, 4805-017 Barco GMR, Portugal. E-mail: miguel.oliveira@dep.uminho.pt*

weight bearing (Qiu *et al.*, 2003). Impaired function, limited range of motion, stiffness, catching, locking and swelling have been described as the most significant associated problems (van Dijk *et al.*, 2010; Zengerink *et al.*, 2010).

Although some OCDs of the ankle are asymptomatic, these can progress to cartilage degeneration and osteoarthritis, thus being a major concern in orthopaedics (Schachter *et al.*, 2005). In this case, conservative treatment is restricted to stable defects in young patients (Anders *et al.*, 2012). In turn, symptomatic OCDs that extend to bone often require surgical treatment in order to restore physiological joint function and prevent the progression of secondary degeneration (O'Driscoll, 1998). In each clinical situation, the choice of the surgical technique to be employed depends on various factors, such as the size of the lesion, site of injury and activity and age of the patient (Valderrabano *et al.*, 2013; Vasiliadis and Wasiak, 2010). Techniques such as abrasion and drilling are considered by the surgeon only in a few particular cases (Vasiliadis and Wasiak, 2010). Microfracture is a widely used technique and it is considered the treatment of choice for the healing of small OCDs, i.e. not exceeding 1.5 cm^2 (Valderrabano *et al.*, 2013). In this particular condition, the use of mosaicplasty, namely osteochondral autotransplantation, is also supported (Valderrabano *et al.*, 2009).

For larger lesions and/or patients with moderate to high activity, new approaches using techniques inspired by regenerative medicine principles have been applied, showing promising results (Giannini *et al.*, 2008; Giza *et al.*, 2010; Gobbi *et al.*, 2006). One of the most encouraging treatments comprises cell-based therapies, such as autologous chondrocyte implantation (ACI). Based on tissue engineering (TE) techniques, implantation of matrix-associated cells has also been attempted, using stem cells (MASI) or chondrocytes (MACI), either at the ankle or knee (Schneider and Karaikudi, 2009; Zengerink *et al.*, 2010). In fact, TE of the ankle has been attracting a great deal of interest (Correia *et al.*, 2014). Although promising, the MASI approach still requires better control of stem cells chondrogenic differentiation *in vivo* as compared to MACI. Therefore, the latter has been more widely applied. The main advantage of MASI over MACI is that it may require a one-step (Giannini *et al.*, 2009) instead of the two-step procedure, thus eliminating the cost and time-consuming process of culture expansion.

For procedures using chondrocytes, the cells are commonly harvested from the healthy cartilage (Candrian *et al.*, 2010), usually from the ipsilateral knee or from the anterior part of the talus (Baums *et al.*, 2006), and are further expanded *in vitro* (Vasiliadis and Wasiak, 2010). In a second stage, chondrocytes are implanted in the defect directly or after 'seeding' into a three-dimensional (3D) porous matrix or scaffold (Valderrabano *et al.*, 2013; Vannini *et al.*, 2013; Vasiliadis and Wasiak, 2010). However, this technique is frequently associated with pain at the donor site (Reddy *et al.*, 2007; Valderrabano *et al.*, 2009) and is detrimental to the function of the ankle joint (Candrian *et al.*, 2010). Up to 50% incidence of knee pain has been described post-transplant of donor knee–ankle (Reddy *et al.*, 2007; Valderrabano *et al.*, 2009). A convenient approach would be the utilization of chondrocytes isolated from OCDs that are usually harvested during surgery. In fact, it was reported that these chondrocytes can be used in ACI or MACI techniques with good clinical results (Giannini *et al.*, 2005). However, the chondrogenic capacity of chondrocytes isolated from OCDs remains controversial, since it has been reported that the formed tissue contains an inferior amount of glycosaminoglycan and type II collagen and a superior amount of type I collagen (Kuroki *et al.*, 2002), as well as a reduced cartilage-forming capacity (Candrian *et al.*, 2010). Therefore, this approach does not seem to be the most adequate strategy when envisioning the treatment of ankle OCDs, at least for now.

The posterior process of the talus, also known as Stieda's process, can be associated with the syndrome of posterior impingement of the talus, especially in athletes and ballet dancers (Bizarro, 1921; Russell *et al.*, 2010). Its clinical management requires arthroscopic surgery, in which Stieda's process is removed (Park *et al.*, 2013). Also described in the literature is the existence of an accessory bone, the os trigonum, which is associated with the posterior process of the talus and has no defined function. Nevertheless, it has been frequently associated with chronic complaints related to plantar flexion mechanisms (Bizarro, 1921). In the symptomatic posterior ankle impingement syndrome, the removal of these structures has been described and proposed for pain management (Park *et al.*, 2013; Russell *et al.*, 2010). The orthopaedic community assumes that the arthroscopic excision of these structures is not associated with significant morbidity (Chao, 2004). Due to the minimally invasive surgery generally used during its excision (Tey *et al.*, 2007; van Dijk *et al.*, 2000), this tissue could be seen as a potential valuable source of cells for ACI or MACI procedures.

To our knowledge, there are no reports on the biological characterization of the posterior talus process or the os trigonum, so basic studies are greatly needed. This work aims to characterize the posterior process of the talus and os trigonum tissues in order to achieve a new source of viable cells for use in tissue-engineering approaches and treatment of OCDs of the ankle. The biological tissue from six patients who underwent excision of the osteochondral fragments was characterized in terms of tissue architecture, composition of extracellular matrix and cellularity by micro-computed tomography (micro-CT) analysis, immunohistochemistry and histomorphometric analysis, respectively. Moreover, cells isolated from the extracted tissue were evaluated *in vitro*, for up to 21 days of culture, regarding their proliferation ability, viability and occurrence of cell apoptosis by DNA quantification, live/dead and MTS assay and TUNEL reaction method, respectively. Cells were also characterized regarding the expression of specific surface markers by flow cytometry, in order to determine cells phenotype.

DOI: 10.1002/term

2. Materials and methods

2.1. Biological samples

Human tissues were obtained through cooperation protocols established with Centro Hospitalar Póvoa do Varzim and do Dragão. The study was approved by the Ethical Committee of Centro Hospitalar Póvoa do Varzim and the University of Minho. The ankle tissues comprising the posterior process of the talus (SP), os trigonum (OT) and normal ankle articular cartilage (AJ) (see supporting information, Figure S1) were obtained from different age and sex donors by means of surgical technique. It was guaranteed that patients were enrolled for surgery (excision of osteochondral fragment) regardless of study participation. Patients received information about the procedure and were selected to participate in the study after obtaining their informed consent in written form. There was no interference in the ordinary course of treatment. Biological samples ($n = 6$) were then selected for tissue ($n = 3$) and cellular ($n = 3$) characterization. The samples were classified as OT or SP, as indicated by the surgeon. One of the samples was obtained from the AJ, and it was also processed for biological characterization according to the established protocols for OT and SP. The tissue was maintained in a phosphate-buffered saline (PBS; Sigma) solution containing 1% v/v antibiotic–antimycotic mixture (AB; Gibco) and processed within 24 h for cell isolation. For studying tissue architecture and histological studies, the extracted tissues were rinsed with PBS and fixed in 10% v/v formalin (Bio Optica) for at least 1 day.

2.2. Tissue characterization

2.2.1. Micro-computed tomography (micro-CT) analysis

The microstructure of the extracted tissues ($n = 3$) was qualitatively and quantitatively evaluated by micro-CT analysis. The structure of the sample was acquired by X-ray and then reconstructed and analysed. Hard/soft tissues (approximately corresponding to bone and cartilage, respectively) morphometric parameters, such as porosity, mean pore size, trabecular thickness and hard/soft tissues profiles, were determined. A 3D reconstruction was also performed in order to characterize the tissue. Data acquisition was performed in a SkyScan 1072 scanner with a pixel size of 16 μm and an integration time of 1280 ms. The X-ray source was set at 82 kV and 122 μA. Approximately 600 projections were acquired over a rotation range of 180°, with a rotation step of 0.45°. Datasets were reconstructed using standardized cone-beam reconstruction software (NRecon v. 1.6.6.0, SkyScan). The output format for each sample was bitmap images. The set of images was orientated with DataViewer (v. 1.4.4, SkyScan) to obtain all samples in the same axis. A representative dataset of the slices was segmented into binary images with a dynamic threshold of 40–120 for soft tissue and 120–255 for hard tissue analysis (grey values). Afterwards, the binary images were used for morphometric analysis (CT Analyser, v. 1.12.0.0, SkyScan) and to obtain the 3D models (CT Vox, v. 2.3.0 r810, SkyScan).

2.2.2. Histological and immunohistochemical characterization

Specimens ($n = 3$) were decalcified with 10% v/v formic acid (Panreac) for 2 weeks. After this step, the samples were processed in a spin tissue processor (STP120-2, Thermo Scientific) overnight, which included immersion in baths of formalin, ascending series of ethanols (Panreac), xylene (VWR International) and paraffin impregnation (Thermo Scientific). The specimens were then embedded in paraffin and sectioned into 3 μm slices using a microtome (HM 355 S, MICROM International GmbH). Three different stainings were performed: haematoxylin and eosin (H&E), Masson's trichrome (MT) and toluidine blue (TB). H&E was used to visualize the tissue structure and architecture, as well as cellularity. MT and TB were performed to detect articular cartilage extracellular matrix components, such as collagen and glycosaminoglycans, according to previously described methods (van Dijk *et al.*, 2000). Slides were then imaged under transmission microscopy through an Axio Imager.Z1m light microscope (Zeiss) with an attached digital camera, AxioCam MRc5 (Zeiss), connected to ZEN blue image processing software (Zeiss). For immunohistochemistry, sections were blocked with sodium citrate buffer (10 mM sodium citrate in 0.05% Tween 20; Aldrich) and stained with the respective two primary antibodies and fluorescent-labelled secondary antibody (see supporting information, Table S1). Counterstaining of cell nuclei was further performed with 4,6-diamidino-2-phenyindole, dilactate (DAPI, Sigma). Sections were imaged under fluorescence microscopy using an AxioCam MRc5 digital camera (Zeiss) connected to ZEN blue image processing software (Zeiss) attached to the Axio Imager.Z1m light microscope (Zeiss).

2.2.3. Histomorphometric analysis

The images obtained from the slides stained with H&E were used to perform a histomorphometric analysis to determine the chondrocyte density on cartilage segments. The WCIF ImageJ software program (US National Institutes of Health) was used for cell counting. After subtracting the background, a 12-radius threshold was used to reduce background noise and automatic cell counting (nuclei) was performed. A total of 50 photomicrographs ($700 \times 500\ \mu m^2$)/specimen were analysed ($n = 3$).

DOI: 10.1002/term

2.3. Cells biological characterization

2.3.1. Cell isolation and expansion

Chondrocytes populations ($n = 3$) were isolated following an enzymatic digestion-based method with type II collagenase (Sigma) from ankle tissues. The extracted tissue was placed in PBS solution and washed several times with PBS containing 1% v/v AB mixture, until total removal of blood or other bodily contaminants was achieved. Cartilage tissue was then separated from bone and, after being washed several times with PBS solution containing 1% v/v AB mixture, the cartilage portion was cut into small pieces. Tissue digestion was performed by incubation at 37 °C in a humidified atmosphere of 5% CO_2 for 1–2 h in 10–20 ml of a mixture composed of Dulbecco's modified Eagle's medium F12 (DMEM F12; Gibco), supplemented with 10% fetal bovine serum (FBS; Gibco), 1% AB mixture and type II collagenase (1:1). The digested tissue was filtered and the cell suspension centrifuged at 1220 rpm for 5 min. The isolated cell populations were expanded in DMEM F12 supplemented with 10% FBS and 1% AB mixture until confluence was reached. Chondrocytes were expanded until passage 3 and detached from the T-75 culture flask using TrypLE Express (Gibco). Polystyrene tissue culture was performed in a 24-well plate, using cells at passage 4 with a cell density of 10 000 cells/well. Each sample was evaluated after specific periods of culture (time points, TPs), i.e. 1, 3, 7, 14 and 21 days, in triplicate for each tissue type, and three wells without cells were used as control. Two independent sets of experiments were performed.

2.3.2. Cellular viability and proliferation

Cell metabolic activity was assessed by performing MTS [3-(4,5-dimethylthiazol-2-yl)-5(3-carboxymethoxyphenyl)-2(4-sulphofenyl)-2*H*-tetrazolium] assay (Cell Titer 96® Aqueous Solution Cell Proliferation Assay, Promega), according to the ISO/EN 10993 Part 5 guidelines (ISO/EN10993-5, 2009). At each TP (i.e. 1, 3, 7, 14 and 21 days), cultured cells were washed with PBS solution and incubated in MTS reagent at 37°C in a 5% CO_2 atmosphere for 3 h in the dark. After incubation, 100 µl of each well (in triplicate) were transferred into a 96-well plate for optical density (OD) measurement at 490 nm in a microplate reader (Molecular Devices). The percentage of cell viability was calculated after normalization with the mean OD value obtained for the negative control. OD is directly proportional to the cellular activity, being a measure of mitochondrial activity.

Detection and quantification of DNA was performed by using the Quant-i™ PicoGreen® dsDNA Reagent (Invitrogen). After washing the cells with PBS, 1 ml ultra-pure water was added to each well. The cells were then mechanically detached from the well and the suspension was transferred into Eppendorf tubes. After incubation in a water bath at 37°C for 1 h, the cell suspension was frozen at –80°C for at least 1 h. Afterwards, the mixture was defrosted in an ultrasonic water bath (DT100H Sonorex Digitec, Bandelin) for 15 min and transferred in triplicate into a 96-well plate. PicoGreen® solution was added afterwards in a 1:1 ratio. Fluorescence was measured in a microplate reader at ex/em ~480/520 nm. λDNA (Invitrogen) was used to prepare the standard curve.

Cell viability was evaluated by live/dead assay after culturing the cells in 13 mm tissue culture coverslips. Live cells (stained with calcein AM 2:1000, Gibco; ex/em ~495/515 nm) and dead cells (indicated by propidium iodide 1:1000, Gibco; ex/em ~495/635 nm) were imaged through a Zeiss Axio Imager.Z1m fluorescence microscope.

2.3.3. Cellular apoptosis

The *in situ* Cell Death Detection Kit (Roche) was used to detect apoptotic cells, using the terminal deoxynucleotidyl transferase dUTP nick end labelling (TUNEL) reaction. Briefly, cells cultured in 13 mm tissue culture coverslips were washed in PBS and fixed in 10% v/v formalin for 1 h at room temperature. Afterwards, the cells were incubated in a permeabilization solution (0.1% Triton X in 0.1% in sodium citrate, Sigma) for 2 min on ice. Negative (without terminal transferase) and positive (with DNase I recombinant 20 U/ml; Amresco) controls in 50 mM Tris(hydroxymethyl) aminomethane (Sigma), pH 7.5, and 1 mg/ml bovine serum albumin (Sigma) were also prepared. For each sample, 50 µl TUNEL reaction mixture was added and incubated at 37°C, 5% CO_2 for 1 h in the dark, as well as on the positive and negative controls. Counterstaining with fluorescein phalloidin (Sigma) and DAPI was also performed. Apoptotic cells were imaged using a Zeiss Axio Imager.Z1m fluorescence microscope (ex/em ~495/515 nm) and phalloidin (ex/em ~540/565 nm) and DAPI (ex/em ~358/461 nm) were used to double-check the location of cells and their nuclei.

2.3.4. Matrix production evaluation

Evaluation of matrix production was performed by toluidine blue O (Betalab) staining at 1% w/v in cells grown in 13 mm tissue culture coverslips for each period of culture. Images were obtained under transmission microscopy through an Axio Imager.Z1m light microscope.

2.3.5. Phenotype characterization

Fluorescence-activated cell sorting (FACS) analysis was performed to examine surface marker expression on chondrocytes at passages 2 and 3 following isolation from cartilage samples ($n = 3$). Cells were tested using anti-human monoclonal fluorescein isothiocyanate (FITC)-conjugated mouse CD105 (AbD Serotec), CD90 and CD45 (BD Biosciences) antibodies; phycoerythrin (PE) conjugated mouse CD73, CD44 and CD34 (BD Biosciences) antibodies; and allophycocyanin (APC)

DOI: 10.1002/term

conjugated rat CD49f (eBioscience) and mouse CD90 (BD Biosciences) antibodies. All antibodies were used at concentrations recommended by the manufacturers for FACS analysis. Briefly, cells frozen at different passages were thawed, collected in culture media and counted using the trypan blue exclusion method. A cell suspension containing a total of 6×10^5 cells was centrifuged for 5 min at $300 \times g$ and the pellet was resuspended in 500 µl PBS containing 2% w/v BSA (Sigma). For direct staining, 1.5×10^5 cells/tube were incubated for 15 min with fluorochrome-conjugated antibodies at room temperature in the dark. After incubation, the cells were washed with PBS/BSA solution, centrifuged for 5 min at 1500 rpm, resuspended in PBS and analysed with counting of a minimum of 40 000 events. Calibrite beads three-colour kit (BD CaliBRITE™ beads, BD Biosciences) was used to adjust the equipment instrument settings before running the samples. The data were acquired using a BD FACSCanto™ (BD Biosciences) flow cytometer. Labelling experiments were repeated three times.

2.4. Statistical analysis

Statistical analysis was performed using commercial SPSS software (IBM SPSS Statistics v. 21.0, IBM). ANOVA Bonferroni was used to assess significant differences in the mean values of cell counting on each sample. Paired samples *t*-tests were used to evaluate significant differences in the mean values of absorbance/DNA concentration between time points. Complementarily, Cohen's *d*-test was used. Significant differences between samples were assessed with ANOVA Bonferroni. In all cases, the level of significance used was set at $p < 0.05$ for a 95% confidence interval.

3. Results

3.1. Tissue characterization

Two samples of the posterior process of the talus (SP) and one of the os trigonum (OT) explants were characterized by micro-computed tomography (micro-CT) analysis and histology/immunohistochemistry, and were designated by SP1, SP2 and OT, respectively. The mean age of the patients was 38 ± 12 years.

The structure of the samples was acquired by X-ray and then reconstructed and analysed. Hard/soft tissues (approximately corresponding to bone and cartilage, respectively) morphometric parameters, such as porosity, mean pore size, trabecular thickness and hard/soft tissues profiles, were determined. A 3D reconstruction was also performed in order to characterize the tissue. The data obtained in micro-CT analysis (Table 1) indicated values of porosities for OT, SP1 and SP2 of 90%, 93% and 98% in hard tissue and 68%, 77% and 76% in soft tissue, respectively. Mean trabecular thickness in hard tissue was 242, 214 and 162 µm for OT, SP1 and SP2, respectively. In soft tissue, the values of mean trabecular thickness were 278, 177 and 251 µm for OT, SP1 and SP2, respectively. Similarly to the parameter of mean porosity, the pore size was larger in hard tissue in all samples. For all specimens, the cartilage tissue represented at least 20% on average. The OT has a higher percentage of cartilaginous tissue, i.e. 32% as compared to SP1 and SP2. Interconnectivity was higher in hard tissue as compared to soft tissue.

Table 1. Structural properties of hard and soft tissues in three ankle explants

	OT	SP1	SP2
Hard tissue/bone			
Mean porosity (%)	90	93	98
Mean trabecular thickness (µm)	242	214	162
Mean pore size (µm)	2247	3970	2377
Interconnectivity (%)	92	90	99
Soft tissue/cartilage			
Mean porosity (%)	68	77	76
Mean trabecular thickness (µm)	278	177	251
Mean pore size (µm)	1194	2906	2203
Interconnectivity (%)	79	80	84

OT, os trigonum; SP1 and SP2, Stieda's processes.

Figure 1 shows the micro-CT morphometric analysis of the human ankle explants. All the explants reached approximately a 50% content in soft tissue (Figure 1A). The distribution of hard tissue trabecular thickness (Figure 1B) showed that about 36% of the trabecular diameters were in the range 181.3–280.2 µm. From the data obtained for soft tissue thickness (Figure 1B), it was possible to observe that around 22% of the diameters were in the range 155.4–181.3 µm, which indicated that soft tissue presents inferior trabecular diameters as compared to hard tissue. In terms of hard tissue pore size, the profile showed that the majority of the pores had diameters > 80–110 µm. Compared with hard tissue pore size, a higher variation in pore size values was found in soft tissue for all explants. Moreover, soft tissue appeared to have two types of pores: a smaller range < 10 µm and a larger range of pores that started at approximately 50 µm and reached > 100 µm. Figure 2 shows 2D (X-ray) and 3D reconstructed images of the human ankle OT and SP explants. It is possible to observe two distinct regions, corresponding to cartilage (external part) and bone (core region) tissues.

Figure 3 shows optical microscopy images with different staining for each specimen. H&E staining was used to visualize the tissue structure and architecture, as well as cellularity; MT and TB staining revealed the presence of negatively charged glycosamicoglycans and proteoglycans within the cartilage. The deposition of type II collagen was also detected on cartilage tissue by immunohistochemical analysis. Although the presence of type I collagen was also evaluated (see supporting information, Figure S2), it was not possible to be detected, due to the natural fluorescence of the specimens.

The quantification of cells in SP and OT was performed using WCIF ImageJ software, in order to evaluate chondrocyte density within the cartilage in this kind of tissue.

DOI: 10.1002/term

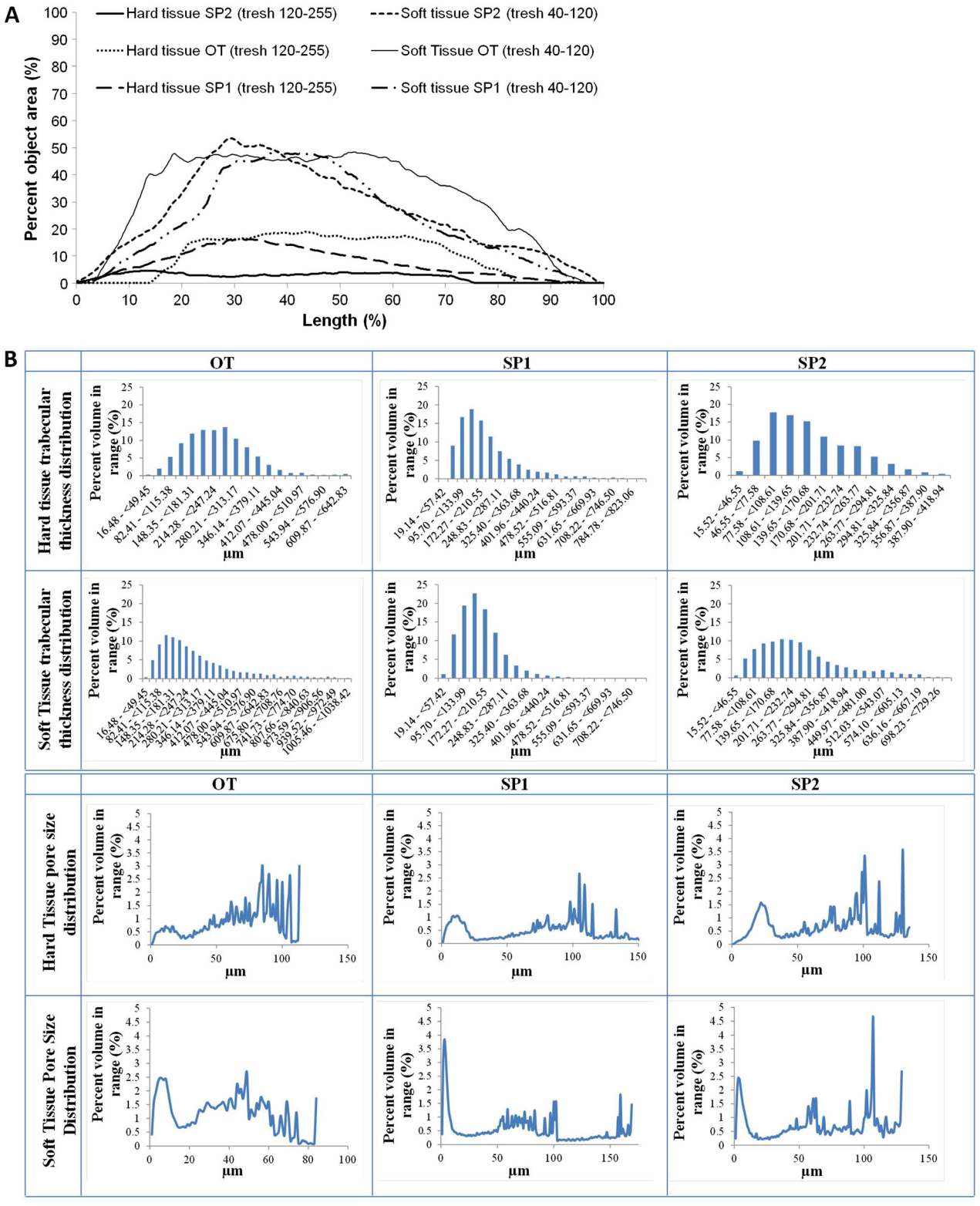

Figure 1. Micro-CT morphometric analysis of human ankle explants: (A) percentages of soft and hard tissue; (B) trabeculae and pore size distributions in the hard and soft tissue of the explants; OT, os trigonum; SP, Stieda's process

Cell density observed in cartilage had a mean value of 350 ± 101 cells/mm^2 for OT, 204 ± 65 cells/mm^2 for SP1 and 342 ± 76 cells/mm^2 for SP2 (see supporting information, Figure S3). Significant differences were observed in average cell counts/mm^2 between SP1 and SP2, as well as between SP1 and OT ($p < 0.001$). No significant differences were observed between SP2 and OT ($p > 0.5$).

3.2. Cells biological characterization

The ages of tissue donors for cell isolations were 35 (SP), 19 (OT) and 23 (AJ) years, with an average age of 26 ± 7 years. The enzymatic method used for chondrocytes isolation from the ankle tissues proved to be reliable, as it consistently permitted to obtain

DOI: 10.1002/term

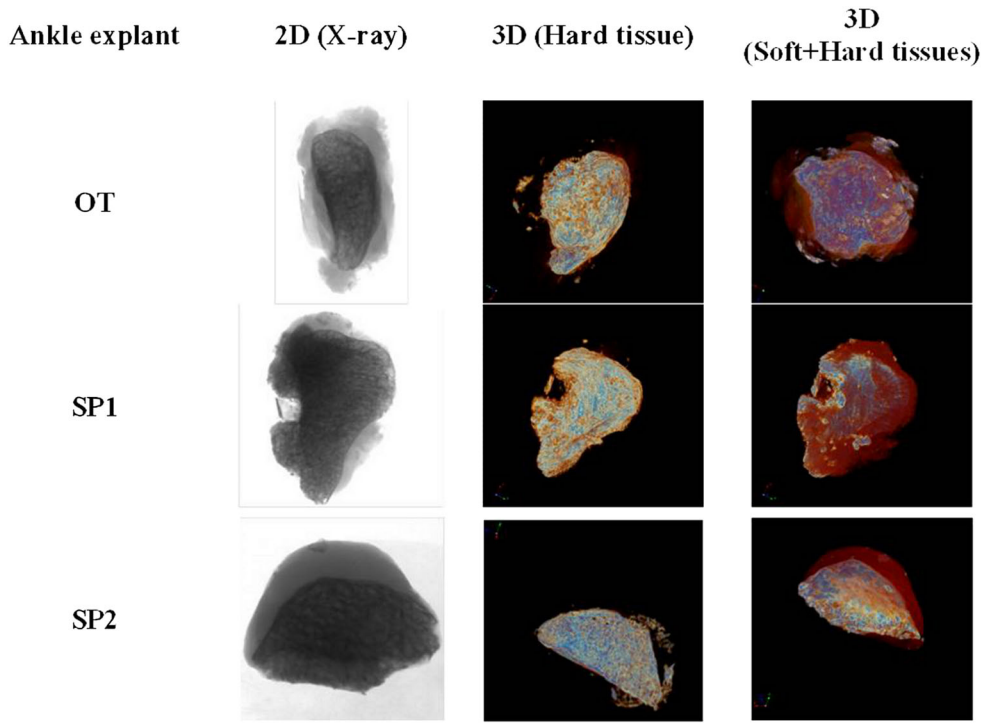

Figure 2. 2D and 3D images of human ankle explants obtained by micro-CT analysis; OT, os trigonum; SP, Stieda's process

viable cells. Isolated cells presented a round morphology typical of chondrocytes. At passage 4, cells cultured for different time periods (i.e. 1, 3, 7, 14 and 21 days) exhibited a similar elongated and spindle-shaped morphology characteristic of dedifferentiated chondrocytes.

The metabolic activity of the isolated chondrocytes was quantified by reduction of MTS reagent at each culture time for the three types of tissue (Figure 4A). The results showed that cells remained metabolically active at each time point (TP) tested. For each sample, differences between two consecutive TPs were significant ($p < 0.05$), except for TP_14d–TP_21d (d = days) on the AJ sample, where no significant differences were observed. Within each TP, significant differences were observed between each type of cell in most cases ($p < 0.05$). Cell proliferation was evaluated through quantification of DNA of the cultured cells at each period of culture (Figure 4B). The DNA concentration increased significantly along the culture period, except on TP_21d of the OT sample, where a significant decrease was observed ($p < 0.001$). Significant differences were observed between the three samples tested for all the periods of culture, except on TP_1d between SP and AJ and TP_21d between SP and OT, where no significant differences were observed ($p > 0.05$).

Live/dead imaging of the different groups corroborated the viability (MTS) and proliferation (DNA quantification) studies, as viable cells (green fluorescence) were observed by fluorescence microscopy (Figure 5). The number of viable cells increased from day 1 until day 21 of culture.

Cellular apoptosis was investigated by means of performing TUNEL assay (Figure 6). This study also corroborated the live/dead findings, as no apoptosis was visualized, i.e. no green fluorescence (upper right images) was observed for the great majority of the cells at each culture time.

Matrix production and deposition (i.e. proteoglycans and collagen) was also evaluated with TB staining in each period of culture for each specimen. No relevant matrix deposition was observed from day 1 until day 21 in all types of cells (Figure 7).

For performing phenotypic characterization, ankle chondrocytes were isolated from tissue harvested from three independent donors (mean age 26 ± 7 years). Cells were cultured until reaching confluence and trypsinized at passages 2 and 3. Subsequently the cell population was analysed for surface antigens by flow cytometry. Flow-cytometer calibration was based on autofluorescent expression of FITC, APC and PE by isolated chondrocytes. The cells do not express their own fluorescence at any of the channels used, as confirmed in Figure 8A for FITC and representative for the APC and PE channels. Fluorescent distribution of the different chondrogenic and MSC surface markers was evaluated at passages 2 and 3 of cell populations. Figure 8B represents the positive fluorescent distribution of FITC and Figure 8C the absence of fluorescence expression. The surface screening showed that cells maintained expression of the chondrogenic surface markers CD105, CD90, CD73, CD49f and CD44, while showing a very low expression of MSC markers CD45 and CD34, in the living cells between passages 2 and 3, confirming the maintenance of the chondrogenic phenotype of the cells isolated from ankle tissues during culture (Figure 8D).

DOI: 10.1002/term

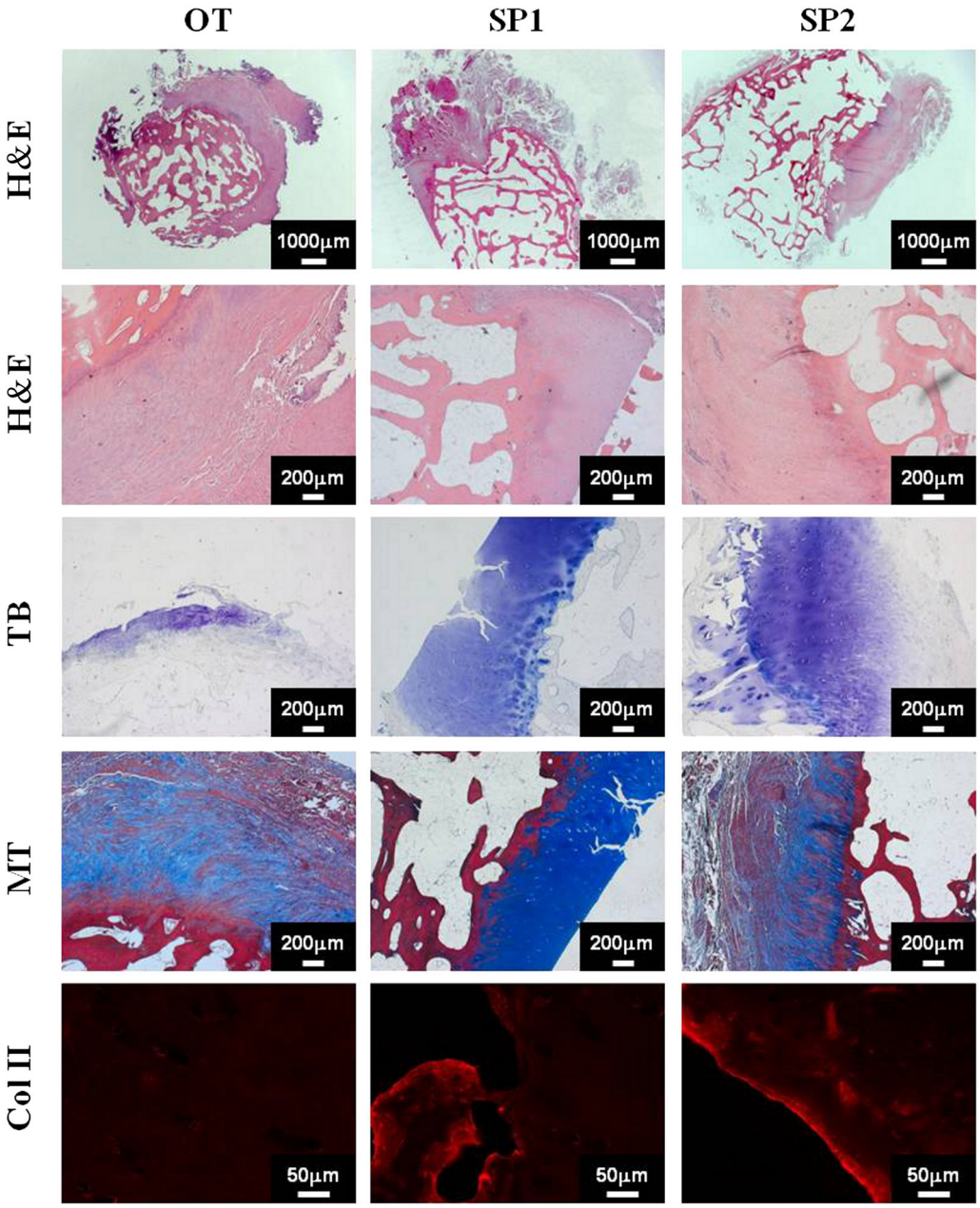

Figure 3. Microscopy images of the histological sections of cartilage: rows 1–4, histological stainings of cartilage extracellular matrix; row 5, immunohistochemical localization of type II collagen; H&E, haematoxylin and eosin; TB, toluidine blue; MT, Masson's trichrome; Col II, type II collagen; OT, os trigonum; SP, Stieda's process

4. Discussion

In this study, the posterior process of the talus (SP), os trigonum (OT) and normal articular ankle cartilage (AJ) tissues and isolated cells were characterized. Cells isolated from SP, OT and AJ were compared in terms of viability and proliferation in 2D cultures, as well as in their post-expansion extracellular matrix-forming capacity.

As previously shown in Figure S1A (see supporting information), the SP and OT structures are closely related to the talus. Characteristically, the OT is not fused to the talus, whereas the SP is described as a prominent elongated posterolateral process of the talus (Rathur *et al.*, 2009). From micro-CT analysis, hard tissue and soft tissue can be associated with bone and cartilage fractions, respectively. In the three explants, cartilage reached approximately 50% of the total tissue content. OT showed a higher content in cartilage tissue as compared to SP. Our results from micro-CT morphometric analysis showed that there is soft tissue completely surrounding the hard tissue. Nevertheless, all the explants presented high amounts of cartilage, which supports the hypothesis in our study. Our findings were corroborated by the histological studies, where staining by MT and TB denoted the presence of cartilage-like matrix. In SP1, the blue staining was more intense than in SP2 and OT. It was also possible to observe the appearance of typical hyaline cartilage, with isolated and rounded chondrocytes surrounded by the cartilaginous extracellular matrix

DOI: 10.1002/term

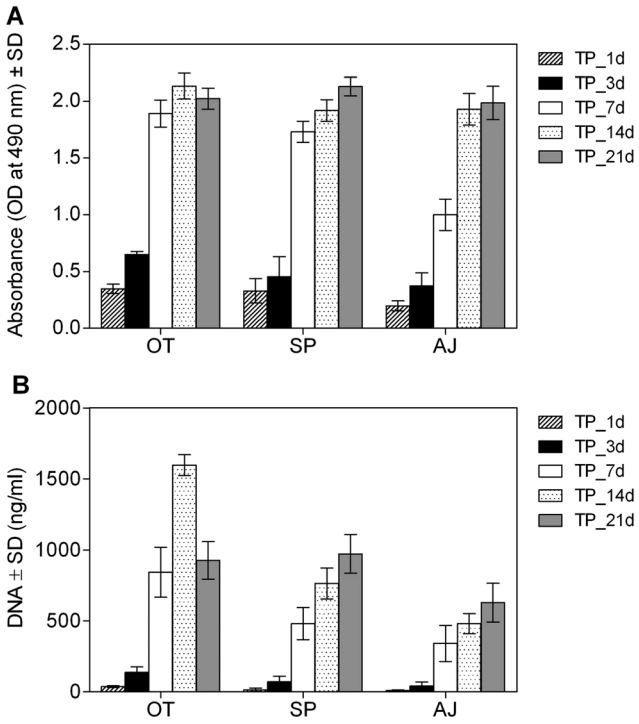

Figure 4. Evaluation of biological performance of cells isolated from ankle tissues and cultured for 1, 3, 7, 14 and 21 days (d). (A) Evaluation of cell viability: statistically significant differences were observed between time points for each sample ($p < 0.05$, $d > 0.8$). (B) Assessment of DNA content: statistically significant differences were observed between time points for each sample ($p < 0.001$, $d > 0.8$); OT, os trigonum; SP, Stieda's process; AJ, ankle joint; TP, time point

(Junqueira *et al.*, 2007). On the other hand, OT and SP2 were showed to possess less hyaline cartilage content. Fusiform chondrocytes interspersed with collagen fibres were observed in OT and SP2, which is typical of fibrocartilage. This type of cartilage presents mainly type I collagen fibres instead of the characteristic type II collagen of hyaline cartilage. Nevertheless, type II collagen was found in all characterized explants, as demonstrated by immunohistochemical analysis. While no considerations could be made based on these results regarding type I collagen deposition, it is not possible to conclude that SP2 and OT present higher amounts of fibrocartilaginous tissue. SP and OT did not possess higher amounts of hyaline cartilage, which was expected, since these tissues are not anatomically confined to an articular area, where hyaline cartilage is indicative of healthy articular cartilage. Despite the type of cartilage present in OT or SP, the presence of viable chondrocytes supports the study hypothesis. Several other studies have reported the ability of chondrocytes to produce hyaline matrix, i.e. deposition of glycosaminoglycans and type II collagen, under chondrogenic medium and in the presence of growth factors (Giannini *et al.*, 2005; Tay *et al.*, 2004). It is known that during monolayer expansion, chondrocytes undergo a process of dedifferentiation, acquiring a fibroblast-like phenotype and exhibiting a certain degree of plasticity, being able to differentiate towards the chondrogenic phenotype in response to specific microenvironmental factors (Barbero *et al.*, 2006; Benya and Shaffer, 1982).

Once again, in histomorphometric analysis, the average number of cells/mm^2 in SP1 was significantly different ($p < 0.001$) as compared to SP2 and OT. This corroborates the assumption of a larger amount of hyaline cartilage in SP1 explants, contrarily to SP2 and OT, where no significant differences ($p > 0.05$) were observed. Due to the typical wide matrix deposition that occurs in hyaline cartilage, the cells are more widely spaced, which determines a lower cell number/mm^2 tissue. Despite the observed differences in cell numbers for the two tissues, a significant number of cells/area of tissue was observed and can be isolated, supporting the idea that chondrocytes can be obtained in enough number for possible use in regenerative medicine approaches.

In this study, it was also demonstrated that it is feasible to isolate viable chondrocytes from the SP and OT. The *in vitro* studies demonstrated that isolated cells proliferated and remained metabolically active for up to 21 days of culture. In fact, a major increase in viability and proliferation was observed from day 3 to day 7. Moreover, between day 7 and day 14, a significant increase ($p < 0.001$) in viability and proliferation was also observed. As expected, the proliferation was not so expressive at day 21, as a consequence of confluence-induced cell death. A decrease in DNA content was also observed in OT isolated cells at day 21, possibly due to their high proliferation ability, as depicted by the high DNA content observed at day 14. These results thus showed that isolated ankle cells can grow on 2D cell culture and remain viable for at least 21 days. Furthermore, not only the cells were viable, they were also non apoptotic, as demonstrated by the TUNEL assay. The differences observed between SP, OT and AJ in terms of viability and proliferation within each time period, although significant ($p < 0.05$), do not represent a limitation for further use of chondrocytes isolated from these tissues. In fact, DNA content in AJ at day 21 is significantly inferior as compared to SP and OT. Several studies have reported the use of AJ chondrocytes for autologous chondrocyte implantation (ACI) and matrix associated-cells implantation (MACI) strategies, with promising clinical results (Aurich *et al.*, 2011; Correia *et al.*, 2014; Giannini *et al.*, 2008; Giza *et al.*, 2010). Aurich *et al.* (2011) and Giannini *et al.* (2008) reported a significant improvement in all clinical scores after MACI and ACI procedures, respectively, using chondrocytes isolated from AJ. In this study, isolated OT and SP chondrocytes presented better results in terms of viability and proliferation, which indicates that chondrocytes isolated from OT and SP could also be potentially used for MACI and ACI procedures.

In a study comparing chondrocytes obtained from naturally occurring ankle osteochondral defects (OCDs) and AJ cartilage tissue, OCD chondrocytes were less capable of appropriate extracellular matrix production than chondrocytes from unaffected ankle joints (Schachter *et al.*, 2005). Also, a recent study has shown that chondrocytes obtained from the injured zone in the

DOI: 10.1002/term

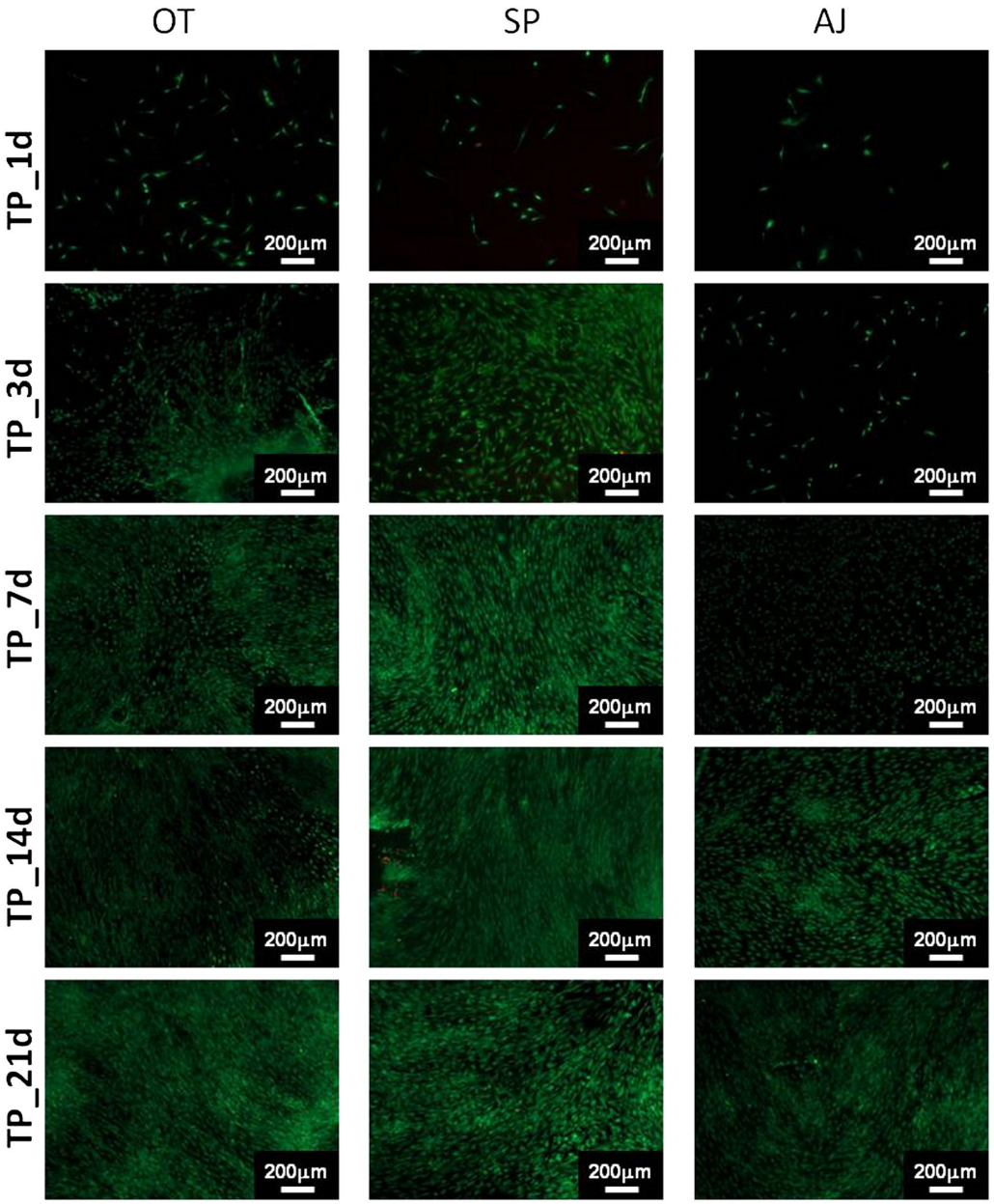

Figure 5. Live/dead imaging of cells isolated from ankle tissues and cultured *in vitro* for 1–21 days (d); OT, os trigonum; SP, Stieda's process; AJ, ankle joint; TP, time point

ankle have inferior regenerative capacities as compared to those from normal tissue, suggesting some reservations concerning their widespread use in the therapeutic field (Candrian *et al.*, 2010). The use of healthy cartilage therefore seems to be more reliable to obtain good clinical results.

In the present *in vitro* studies, standard culture medium was used and no chondrogenic supplements were added. Thus, no relevant matrix production or deposition was observed until day 21, as expected.

Fluorescence-activated cell sorting (FACS) was performed to determine the chondrogenic capacity of the isolated cells, using surface chondrocyte membrane markers (i.e. CD105, CD90, CD73, CD49f and CD44). Because chondrocytes are the main entities for extracellular matrix deposition in cartilage tissue, an alteration in the cellular phenotype has an enormous significance on the type of matrix (Garvican *et al.*, 2008). In the present study, flow-cytometry analysis for cell-surface screening demonstrated that the chondrogenic markers CD105, CD90, CD73, CD49f and CD44 are highly expressed on the surface of isolated ankle human chondrocytes and did not changed their expression during time in culture. On the other hand, the MSCs markers CD45 and CD34 were not detected and the lack of expression was maintained through the culture passages. The present results confirm successful optimization of the protocol for isolation of human chondrocytes from patients' ankles. Moreover, immunocytochemical analysis can be a useful technique for detecting the deposition of matrix, as well as distinguishing whether either of these cells are producing type I or type II collagen during 2D culture. As already

DOI: 10.1002/term

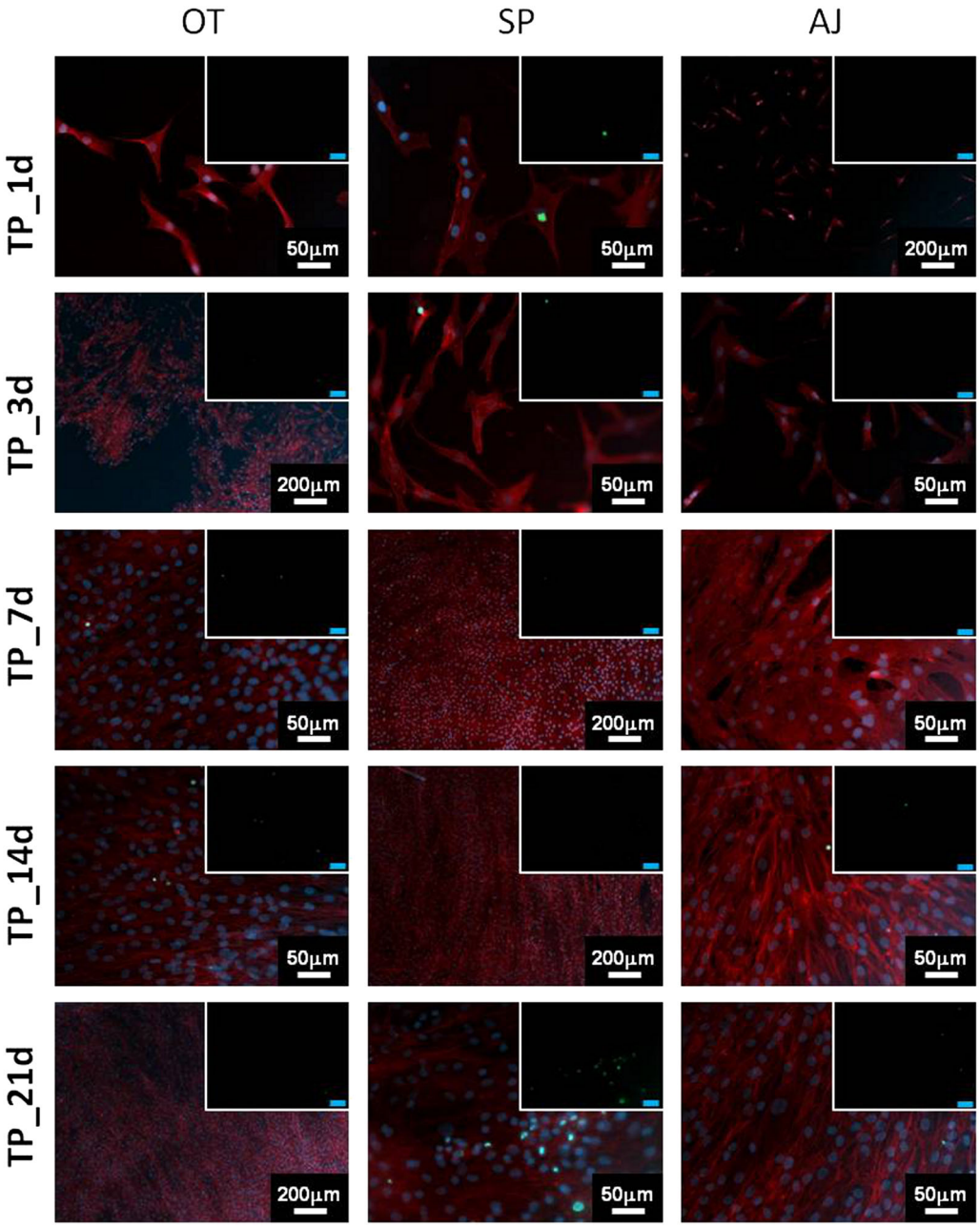

Figure 6. TUNEL assay imaging of cells isolated from ankle tissues and cultured *in vitro* for 1–21 days (d; small images); counterstaining images with phalloidin (cytoskeleton) and DAPI (nuclei) are also shown (large images); OT, os trigonum; SP, Stieda's process; AJ, ankle joint; TP, time point; blue scale bar = 50 µm

stated, the major compounds in hyaline-like cartilage extracellular matrix are type II collagen fibres and glycosaminoglycans. Further studies should be performed in order to evaluate matrix deposition using immunocytochemistry and gene expression by quantitative real-time reverse transcription analysis of relevant markers (e.g. glycosaminoglycans, type I and type II collagen).

It is important to bear in mind that the *in vitro* experimental design to characterize the post-expansion chondrogenic capacity of ankle chondrocytes does not directly allow us to predict the *in vivo* reparative/regenerative ability of the cell types, i.e. if these cells were implanted in the talar lesions, no information is available at this stage to safely assess their biological performance. Thus, subsequent studies are still required prior to *in vivo* use. Experiments comprising the culture of the isolated cells from ST or OT onto a 3D porous matrix in the presence of chondrogenic inducers, either in static or dynamic conditions, and *in vivo* studies using relevant models, are future research directions that need to be pursued as proof-of-concept.

Most of the clinical studies using MACI and ACI procedures have been performed on the knee (Correia *et al.*, 2014), where chondrocytes are usually harvested from healthy cartilage on the ipsilateral side. It has been shown that ankle and knee chondrocytes have similar biosynthetic activities (Candrian *et al.*, 2009). Despite requiring further clinical evaluation, it can be stated that the ankle

DOI: 10.1002/term

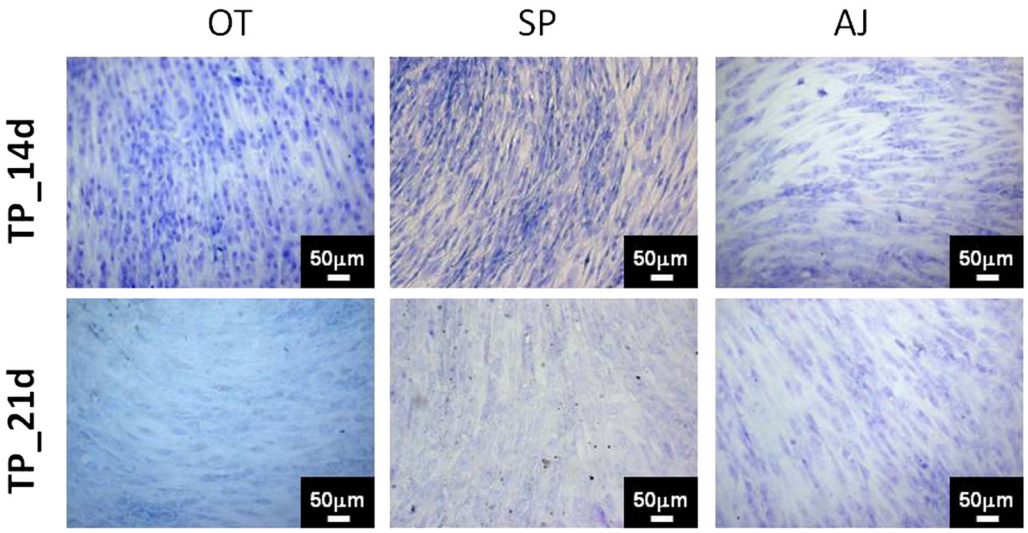

Figure 7. Collagen detection by toluidine blue staining on cells isolated from ankle tissues and cultured *in vitro* for 1–21 days (d). Although only TP_14d and TP_21d had shown positive staining, no relevant detection of collagen was observed throughout the other tested periods (i.e. TP_1d, TP_3d and TP_7d); OT, os trigonum; SP, Stieda's process; AJ, ankle joint; TP, time point

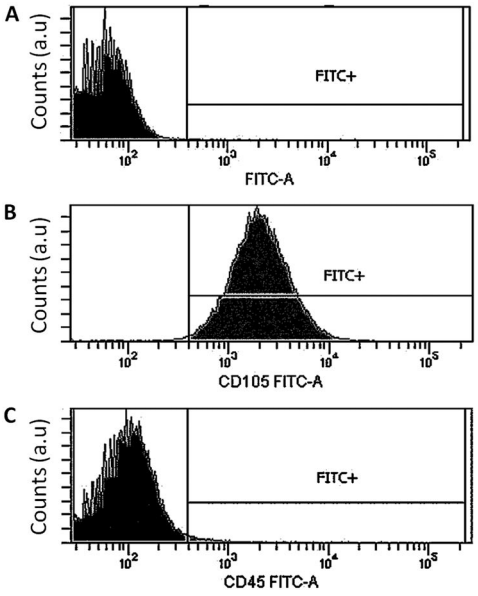

D

Cell Surface Markers		P2-P3 (%) $X \pm S.D.$
Chondrogenic	CD105	87.6 ± 8.8
	CD90	90.8 ± 8.1
	CD73	90.8 ± 8.2
	CD49f	85.3 ± 6.2
	CD44	90.8 ± 8.1
MSCs	CD45	0.6 ± 0.4
	CD34	0.9 ± 1.5

Figure 8. Phenotypic evaluation of cells isolated from ankle tissues by flow cytometry (FCM). Monolayer cultured cells were evaluated for the expression of the human chondrogenic surface markers CD105, CD90, CD73, CD49f and CD44 and the MSC markers CD45 and CD34. (A) FCM histogram for FITC fluorescence calibration showing the absence of autofluorescent expression of FITC by human chondrocytes. (B) FCM histogram showing the fluorescence intensity distribution of CD105–FITC-stained cells. (C) FCM histogram showing the fluorescence intensity distribution of CD45–FITC-stained cells. (D) Percentage of living chondrocytes expressing each analysed cell surface marker. Chondrocytes were obtained from three different donors and were analysed at passages 2 and 3 ($n = 6$ for each cell surface marker; $x \pm SD$, mean ± standard deviation)

can be a source of viable chondrocytes for a possible application in the treatment of cartilage lesions and OCDs in the knee joint.

5. Conclusions

In this study, viable chondrocytes were isolated and cultured from the posterior process of the talus (SP) and the os trigonum (OT). This study points out a new direction by setting up a suitable novel source of chondrocytes (and establishing the methods for isolation and cultivation *in vitro*) that can be potentially used in cell-based and tissue-engineering strategies for the treatment of cartilage and osteochondral lesions. One of the advantages of using this approach, which therefore emphasizes the importance of this study, is that the SP and OT tissues can be obtained by using minimally invasive surgical approaches, thus limiting the side-effects usually related with the classical approaches. The results obtained herein are promising, but further *in vitro* and *in vivo*

DOI: 10.1002/term

preclinical investigations are required to determine the feasibility and safety of this approach prior to its use in clinics.

Conflict of interest

The authors declare no conflicts of interest.

Acknowledgements

The authors are grateful for funds provided by the Portuguese Foundation for Science and Technology (FCT) through the project OsteoCart (Grant No. PTDC/CTM-BPC/115977/2009), as well as the PhD scholarship provided to R. F. Canadas (Grant No. SFRH/BD/92565/2013). The FCT distinction attributed to J. M. Oliveira under the Investigador FCT programme (Grant No. IF/00423/2012) is also greatly acknowledged. The authors are also grateful for funds provided by Fundación MAPFRE (Ayudas a la Investigación Ignacio H. de Larramendi, Prevención, Salud y Medio Ambiente, Spain) under the project 'Preventing the progression of the knee osteoarthritis: advanced therapies combining injectable hydrogels, autologous stem cells and PRP' (Grant No. BIL/13/SA/235). This study was also carried out with the support of Fundo Europeu de Desenvolvimento Regional (FEDER) through Programa Operacional do Norte through the project Articulate (Grant No. 23189).

References

Anders S, Goetz J, Schubert T, *et al*. 2012; Treatment of deep articular talus lesions by matrix associated autologous chondrocyte implantation – results at five years. *Int Orthop* **36**: 2279–2285.

Aurich M, Bedi HS, Smith PJ, *et al*. 2011; Arthroscopic treatment of osteochondral lesions of the ankle with matrix-associated chondrocyte implantation. *Am J Sports Med* **39**: 311–319.

Barbero A, Grogan SP, Mainil-Varlet P, *et al*. 2006; Expansion on specific substrates regulates the phenotype and differentiation capacity of human articular chondrocytes. *J Cell Biochem* **98**: 1140–1149.

Baums MH, Heidrich G, Schultz W, *et al*. 2006; Autologous chondrocyte transplantation for treating cartilage defects of the talus. *J Bone Joint Surg Am* **88**: 303–308.

Benya PD, Shaffer JD 1982; Dedifferentiated chondrocytes re-express the differentiated collagen phenotype when culture in agarose gels. *Cell* **30**: 215–224.

Bizarro AH 1921; On sesamoid and supernumerary bones of the limbs. *J Anat* **55**: 256–268.

Candrian C, Bonacina E, Frueh JA, *et al*. 2009; Intra-individual comparison of human ankle and knee chondrocytes *in vitro*: relevance for talar cartilage repair. *Osteoarthr Cartilage* **17**: 489–496.

Candrian C, Miot S, Wolf F, *et al*. 2010; Are ankle chondrocytes from damaged fragments a suitable cell source for cartilage repair? *Osteoarthr Cartilage* **18**: 1067–1076.

Chao W 2004; Os trigonum. *Foot Ankle Clin* **9**: 787–796.

Correia SI, Pereira H, Silva-Correia J, *et al*. 2014; Current concepts: tissue engineering and regenerative medicine applications in the ankle joint. *J R Soc Interface* **11**: 20130784.

Garvican ER, Vaughan-Thomas A, Redmond C, *et al*. 2008; Chondrocytes harvested from osteochondritis dissecans cartilage are able to undergo limited *in vitro* chondrogenesis despite having perturbations of cell phenotype *in vivo*. *J Orthop Res* **26**: 1133–1140.

Giannini S, Buda R, Grigolo B, *et al*. 2005; The detached osteochondral fragment as a source of cells for autologous chondrocyte implantation (ACI) in the ankle joint. *Osteoarthr Cartilage* **13**: 601–607.

Giannini S, Buda R, Vannini F, *et al*. 2009; One-step bone marrow-derived cell transplantation in talar osteochondral lesions. *Clin Orthop Relat Res* **467**: 3307–3320.

Giannini S, Buda R, Vannini F, *et al*. 2008; Arthroscopic autologous chondrocyte implantation in osteochondral lesions of the talus. *Am J Sports Med* **36**: 873–880.

Giza E, Sullivan M, Ocel D, *et al*. 2010; Matrix-induced autologous chondrocyte implantation of talus articular defects. *Foot Ankle Int* **31**: 747–753.

Gobbi A, Francisco RA, Lubowitz JH, *et al*. 2006; Osteochondral lesions of the talus: randomized controlled trial comparing chondroplasty, microfracture, and osteochondral autograft transplantation. *Arthroscopy* **22**: 1085–1092.

ISO/EN10993–5 2009; Biological evaluation of medical devices. Part 5: Tests for *in vitro* cytotoxicity, Organization IS: Geneva, Switzerland.

Junqueira LC, Carneiro J, Wisse E 2007; Functionele Histologie, 11th edn.Elsevier: Maarssen, The Netherlands.

Kuroki K, Cook JL, Tomlinson JL, *et al*. 2002; *In vitro* characterization of chondrocytes isolated from naturally occurring osteochondrosis lesions of the humeral head of dogs. *Am J Vet Res* **63**: 186–193.

O'Driscoll SW 1998; The healing and regeneration of articular cartilage. *J Bone Joint Surg Am* **80**: 1795–1812.

Park CH, Kim SY, Kim JR, *et al*. 2013; Arthroscopic excision of a symptomatic os trigonum in a lateral decubitus position. *Foot Ankle Int* **34**: 990–994.

Qiu YS, Shahgaldi BF, Revell WJ, *et al*. 2003; Observations of subchondral plate advancement during osteochondral repair: a histomorphometric and mechanical study in the rabbit femoral condyle. *Osteoarthr Cartilage* **11**: 810–820.

Rathur S, Clifford P, Chapman C 2009; Posterior ankle impigemente: os trigonum syndrome. *Am J Orthop* **38**: 252–253.

Reddy S, Pedowitz DI, Parekh SG, *et al*. 2007; The morbidity associated with osteochondral harvest from asymptomatic knees for the treatment of osteochondral lesions of the talus. *Am J Sports Med* **35**: 80–85.

Russell JA, Kruse DW, Koutedakis Y, *et al*. 2010; Patho-anatomy of posterior ankle impingement in ballet dancers. *Clin Anat* **23**: 613–621.

Schachter AK, Chen AL, Reddy PD, *et al*. 2005; Osteochondral lesions of the talus. *J Am Acad Orthop Surg* **13**: 152–158.

Schneider TE, Karaikudi S 2009; Matrix-induced autologous chondrocyte implantation (MACI) grafting for osteochondral lesions of the talus. *Foot Ankle Int* **30**: 810–814.

Tay AG, Farhadi J, Suetterli R, *et al*. 2004; Cell yield, proliferation, and postexpansion differentiation capacity of human ear, nasal and rib chondrocytes. *Tissue Eng* **10**: 762–770.

Tey M, Monllau J, Centenera J, *et al*. 2007; Benefits of arthroscopic tuberculoplasty in posterior ankle impingement syndrome. *Knee Surg Sports Traumatol Arthrosc* **15**: 1235–1239.

Valderrabano V, Leumann A, Rasch H, *et al*. 2009; Knee-to-ankle mosaicplasty for the treatment of osteochondral lesions of the ankle joint. *Am J Sports Med* **37**: 105–111S.

Valderrabano V, Miska M, Leumann A, *et al*. 2013; Reconstruction of osteochondral lesions of the talus with autologous spongiosa grafts and autologous matrix-induced chondrogenesis. *Am J Sports Med* **41**: 519–527.

van Dijk CN, Reilingh ML, Zengerink M, *et al*. 2010; Osteochondral defects in the ankle: why painful? *Knee Surg Sports Traumatol Arthrosc* **18**: 570–580.

van Dijk CN, Scholten PE, Krips R 2000; A two-portal endoscopic approach for diagnosis and treatment of posterior ankle pathology. *Arthroscopy* **16**: 871–876.

Vannini F, Filardo G, Kon E, *et al*. 2013; Scaffolds for cartilage repair of the ankle joint: the impact on surgical practice. *Foot Ankle Surg* **19**: 2–8.

Vasiliadis HS, Wasiak J 2010; Autologous chondrocyte implantation for full-thickness articular cartilage defects of the knee. *Cochrane Database Syst Rev*: CD003323, DOI: 10.1002/14651858.CD003323.pub3.

Zengerink M, Struijs PA, Tol JL, *et al*. 2010; Treatment of osteochondral lesions of the talus: a systematic review. *Knee Surg Sports Traumatol Arthrosc* **18**: 238–246.

Supporting information

Additional supporting information may be found in the online version of this article at the publisher's web-site:

Figure S1. Scheme of the human ankle tissues, identifying the location of Stieda's process, the os trigonum (OT) and SP after arthroscopic excision
Figure S2. Fluorescence microscopy images of Stieda's process (SP1) after immunohistochemical localization of type I collagen, control sample without staining or antibodies and sample treated with type I collagen primary antibody and AlexaFluor 488 secondary antibody
Figure S3. Cartilage cell counting within each sample
Table S1. Primary and fluorescent-labelled secondary antibodies used in immunohistochemical analysis
Supplementary Figures Captions

DOI: 10.1002/term